

Supporting Information

On the mechanism of electrochemical functionalization of carbon nanotubes with different structures with aminophenylphosphonic acid isomers. An experimental and computational approach

Beatriz Martínez-Sánchez^a, Javier Quílez-Bermejo^b, Emilio San-Fabián^a, Diego Cazorla-Amorós^b, Emilia Morallón^a.

^a Departamento de Química Física and Instituto Universitario de Materiales de Alicante (IUMA), University of Alicante, Ap. 99, 03080, Alicante, Spain

^b Departamento de Química Inorgánica and Instituto Universitario de Materiales de Alicante (IUMA), University of Alicante, Ap. 99, 03080, Alicante, Spain

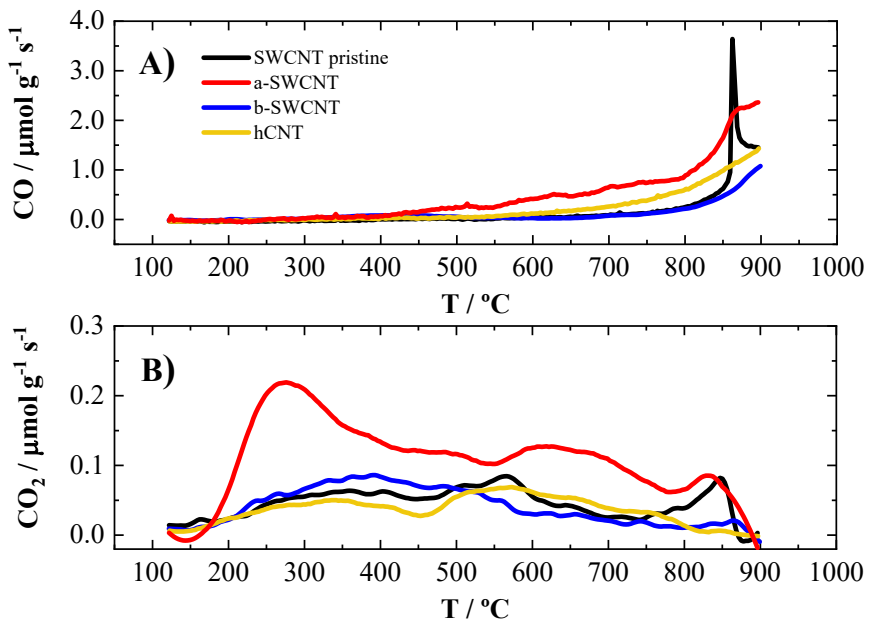


Figure S1. TPD profiles of A) CO and B) CO_2 for SWCNT pristine (black lines), a-SWCNT (red lines), b-SWCNT (blue lines) and hCNT (orange lines) performed in He atmosphere at heating rate of $10^\circ\text{C min}^{-1}$.

Table S1. Chemical composition obtained from the XPS spectra of pristine SWCNT, a-SWCNT, b-SWCNT and hCNT samples. Gravimetric capacity in 0.5 M H₂SO₄ at 50 mV s⁻¹ in N₂ atmosphere.

Sample	O / at. %	N / at. %	Fe / at. %	C / F g ⁻¹
SWCNT pristine	3.13	0.37	0.17	45
a-SWCNT	6.38	0.44	-	63
b-SWCNT	3.28	0.38	0.14	46
hCNT	3.71	-	-	7

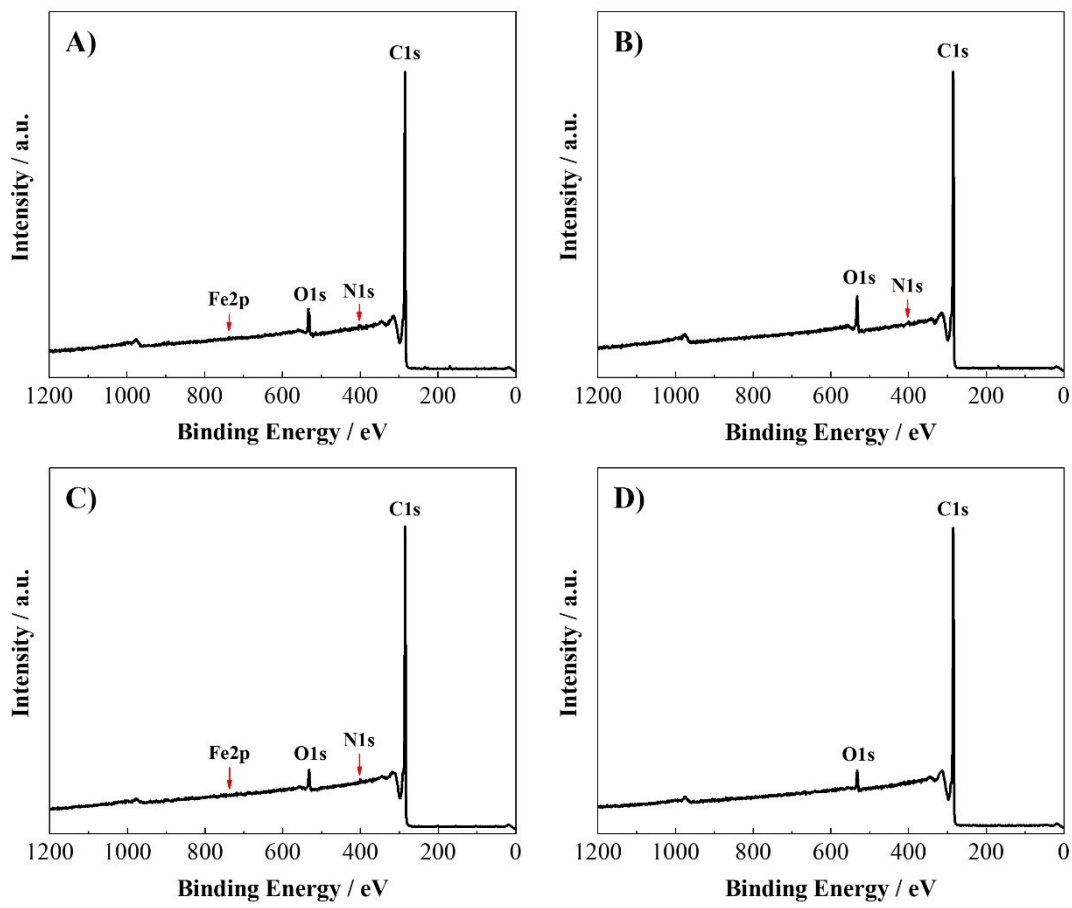


Figure S2. XPS full survey spectra of pristine A) SWCNT, B) a-SWCNT, C) b-SWCNT and D) hCNT samples.

Table S2. Surface chemistry analysis obtained from TPD experiments for the different CNTs.

Sample	CO / $\mu\text{mol g}^{-1}$	CO ₂ / $\mu\text{mol g}^{-1}$	TOTAL O / $\mu\text{mol g}^{-1}$
a-SWCNT	1672	502	2675
b-SWCNT	271	160	592
hCNT	986	164	1314

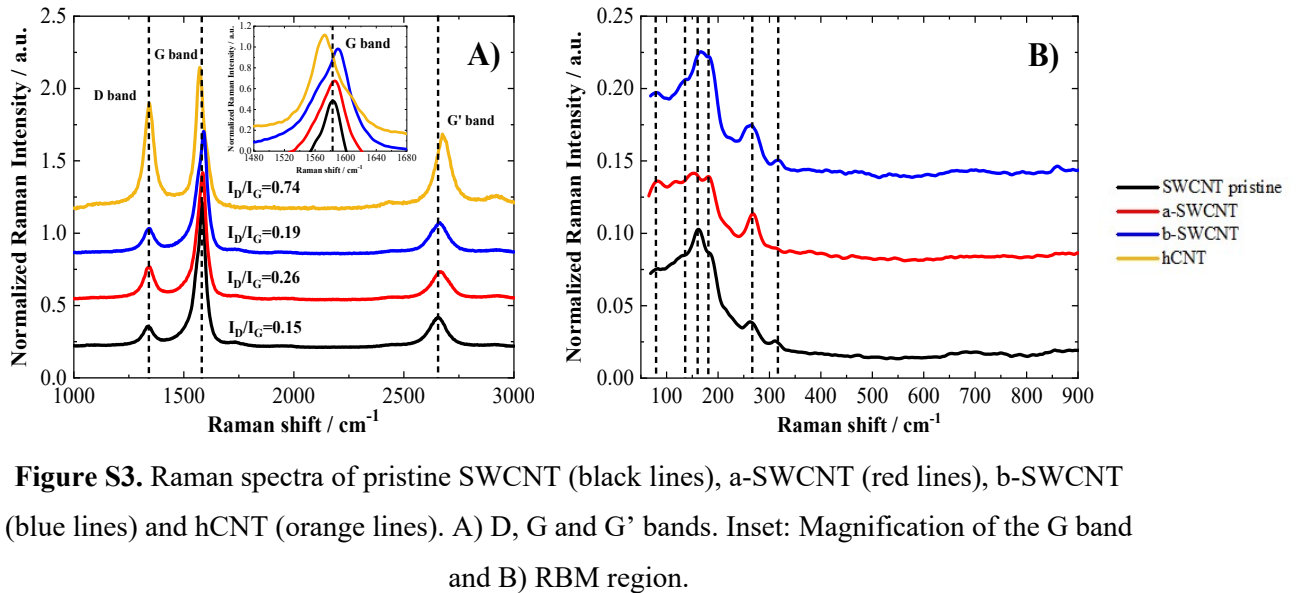


Figure S3. Raman spectra of pristine SWCNT (black lines), a-SWCNT (red lines), b-SWCNT (blue lines) and hCNT (orange lines). A) D, G and G' bands. Inset: Magnification of the G band and B) RBM region.

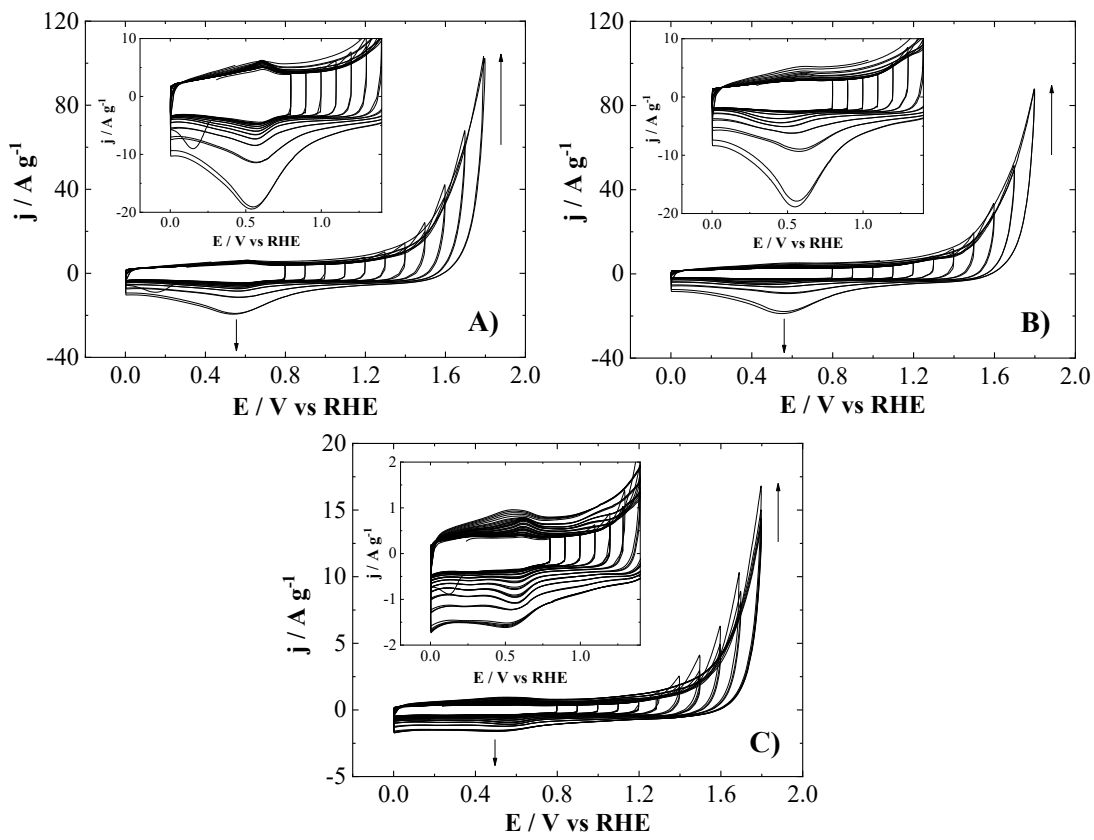


Figure S4. Cyclic voltammograms of the open stepwise upper potential limit from 0.80 to 1.8 V for A) a-SWCNT, B) b-SWCNT and C) hCNT, in 0.5 M H_2SO_4 at 50 mV s^{-1} .

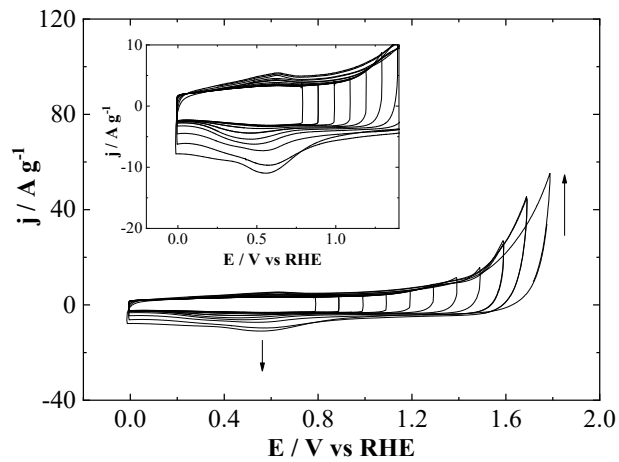


Figure S5. Cyclic voltammograms of the open stepwise upper potential limit from 0.0 to 1.8 V (vs RHE) for pristine SWCNT (unpurified) in 0.5 M H_2SO_4 at 50 mV s^{-1} under N_2 atmosphere.

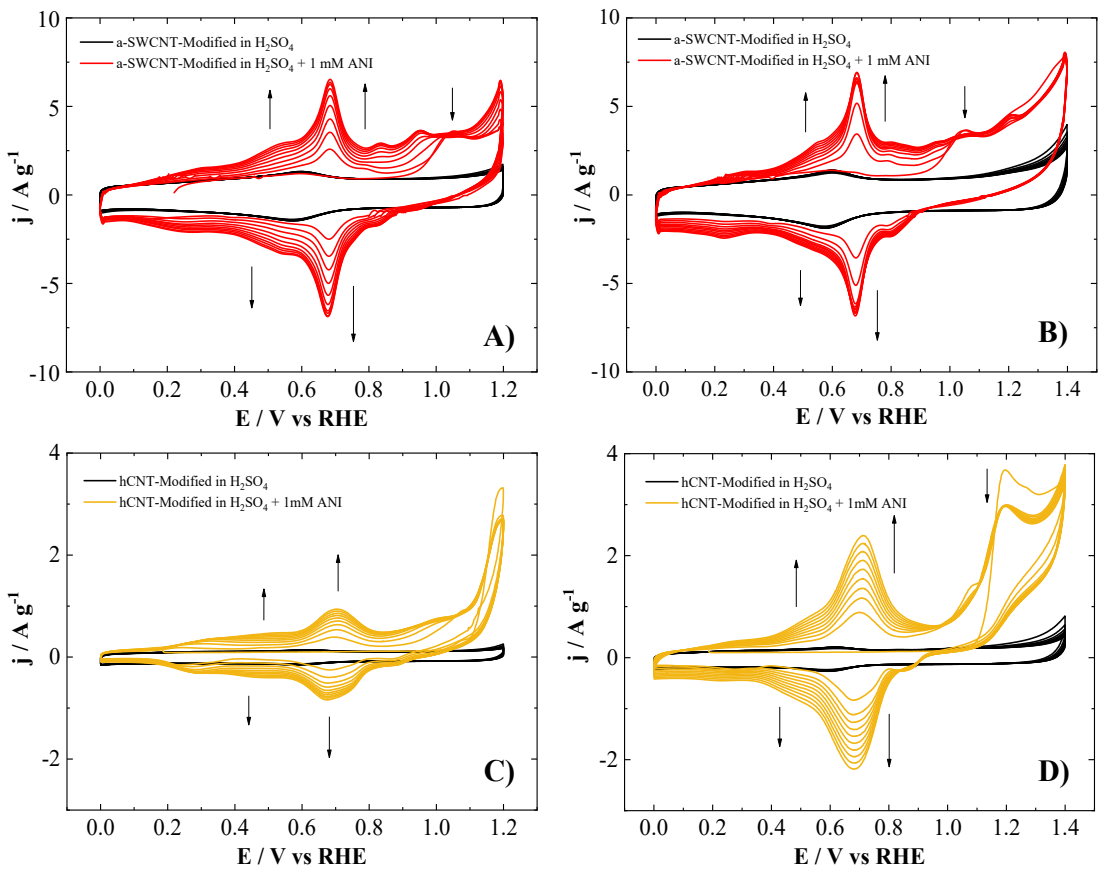


Figure S6. Cyclic voltammograms of the electrochemical functionalization of A, B) a-SWCNT and C, D) hCNT in 0.5 M H_2SO_4 (black lines) and 0.5 M $\text{H}_2\text{SO}_4 + 1 \text{ mM ANI}$ (colored lines) at A, C) 1.2 V and B, D) 1.4 V, during 10 cycles at 10 mV s^{-1} under N_2 atmosphere.

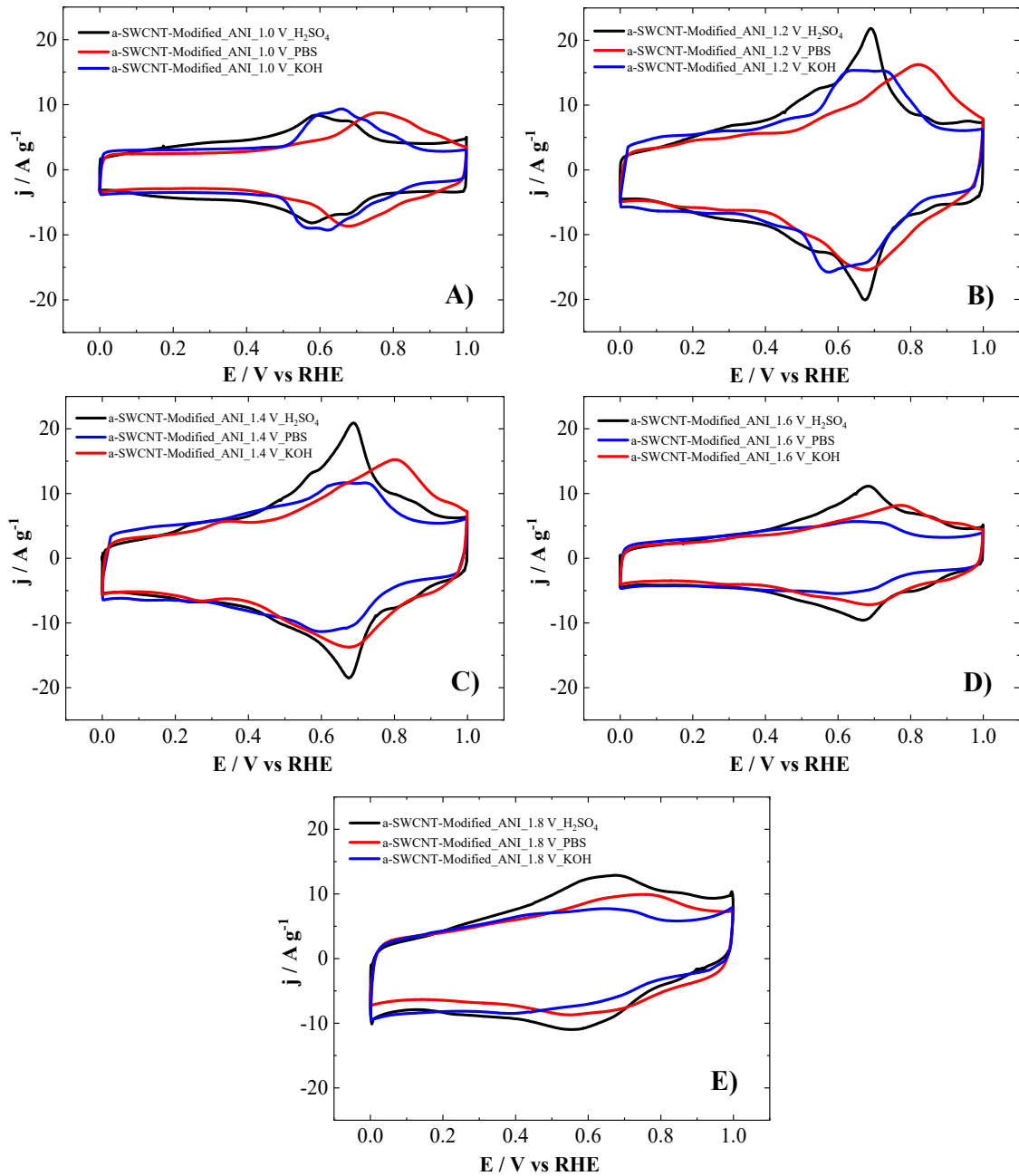


Figure S7. Cyclic voltammograms for a-SWCNT electrochemically modified at A) 1.0 V, B) 1.2 V, C) 1.4 V, D) 1.6 V and E) 1.8 V (vs RHE) with 1 mM ANI, in acid (0.5 M H_2SO_4 , black lines), neutral (0.1 M PBS, pH=7.2, red lines) and alkaline (0.1 M KOH, blue lines) solution free of monomers at 50 mV s^{-1} . 10th cycle.

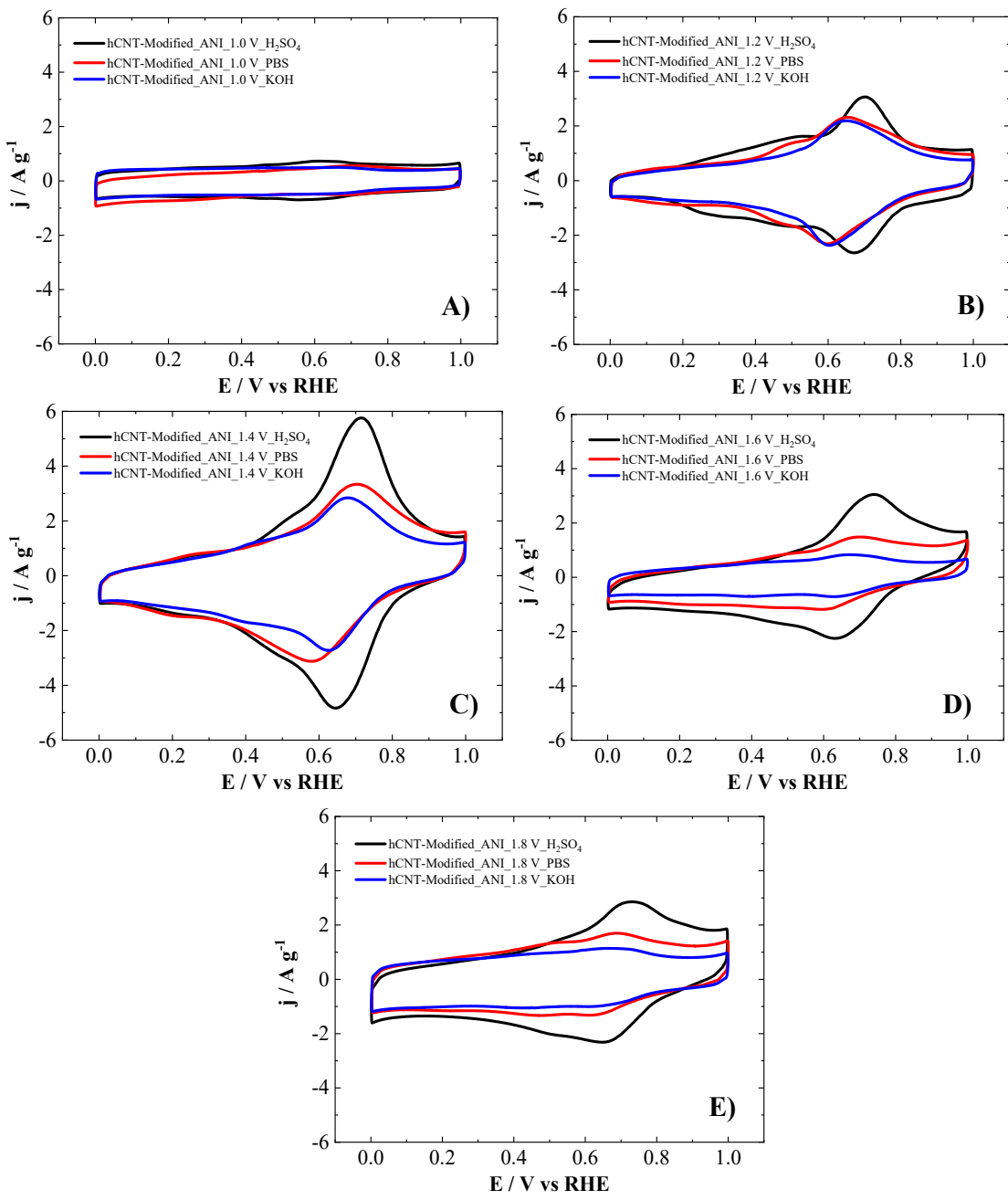


Figure S8. Cyclic voltammograms for hCNT electrochemically modified at A) 1.0 V, B) 1.2 V, C) 1.4 V, D) 1.6 V and E) 1.8 V (vs RHE) with 1 mM ANI, in acid ($0.5 \text{ M H}_2\text{SO}_4$, black lines), neutral ($0.1 \text{ M PBS, pH}=7.2$, red lines) and alkaline (0.1 M KOH , blue lines) solution free of monomers at 50 mV s^{-1} . 10^{th} cycle.

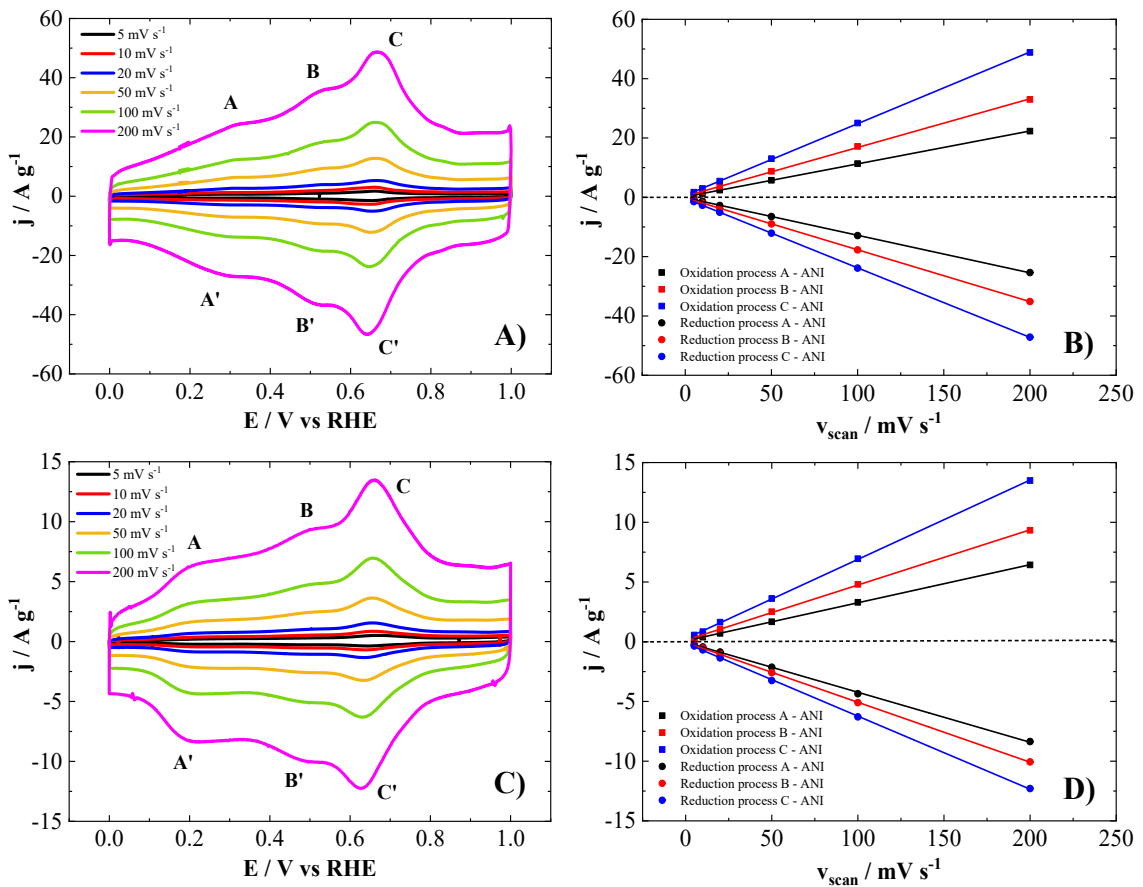


Figure S9. Cyclic voltammograms and correlation of anodic and cathodic current of processes A, B and C vs. v_{scan} (5, 10, 20, 50, 100 and 200 mV s⁻¹) for A, B) a-SWCNT and C, D) hCNT electrochemically modified at 1.2 V (vs RHE) with 1mM ANI, in 0.5 M H₂SO₄ under N₂ atmosphere.

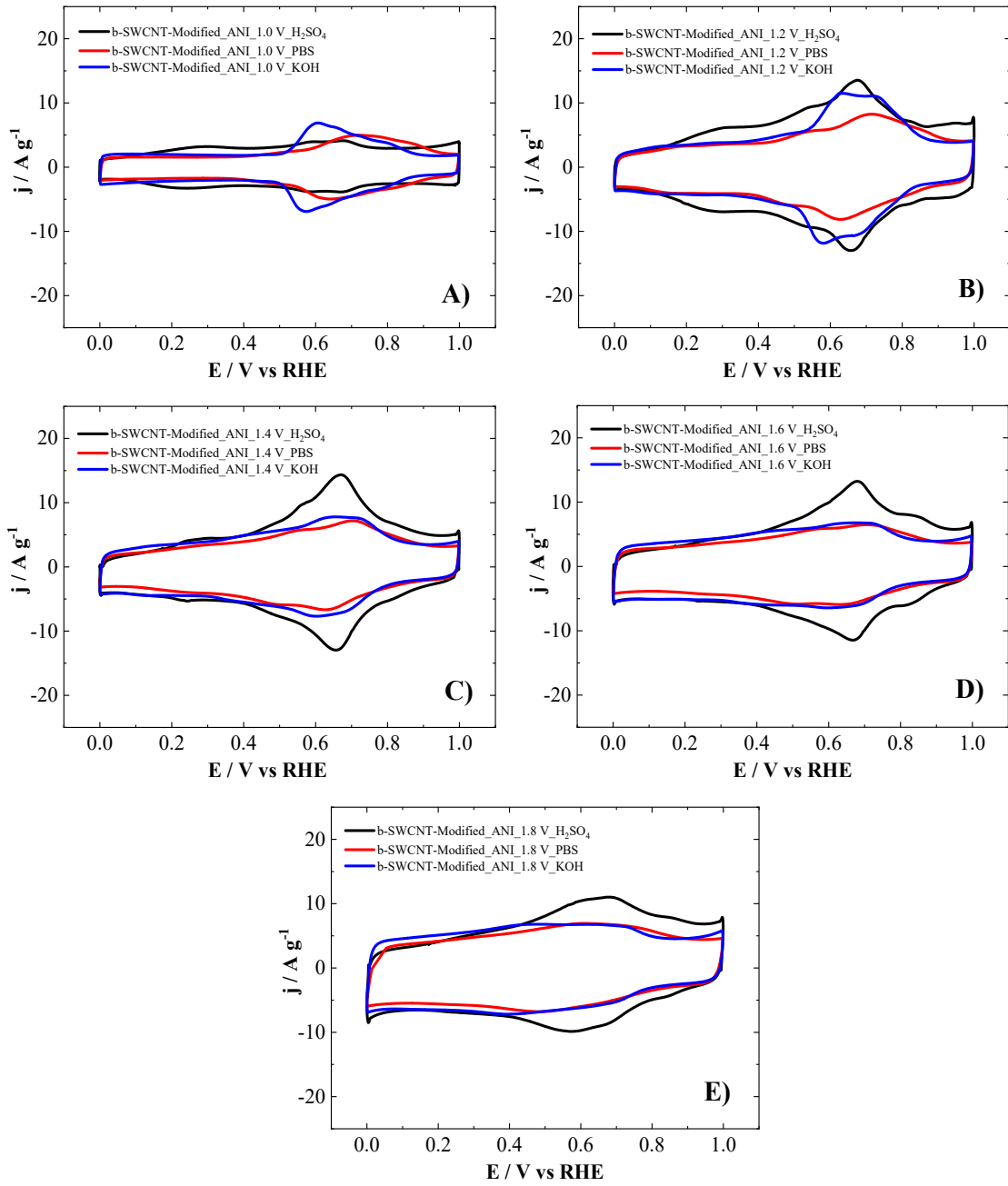


Figure S10. Cyclic voltammograms for b-SWCNT electrochemically modified at A) 1.0 V, B) 1.2 V, C) 1.4 V, D) 1.6 V and E) 1.8 V (vs RHE) with 1 mM ANI, in acid (0.5 M H_2SO_4 , black lines), neutral (0.1 M PBS, pH=7.2, red lines) and alkaline (0.1 M KOH, blue lines) solution free of monomers at 50 mV s^{-1} under N_2 atmosphere. 10th cycle.

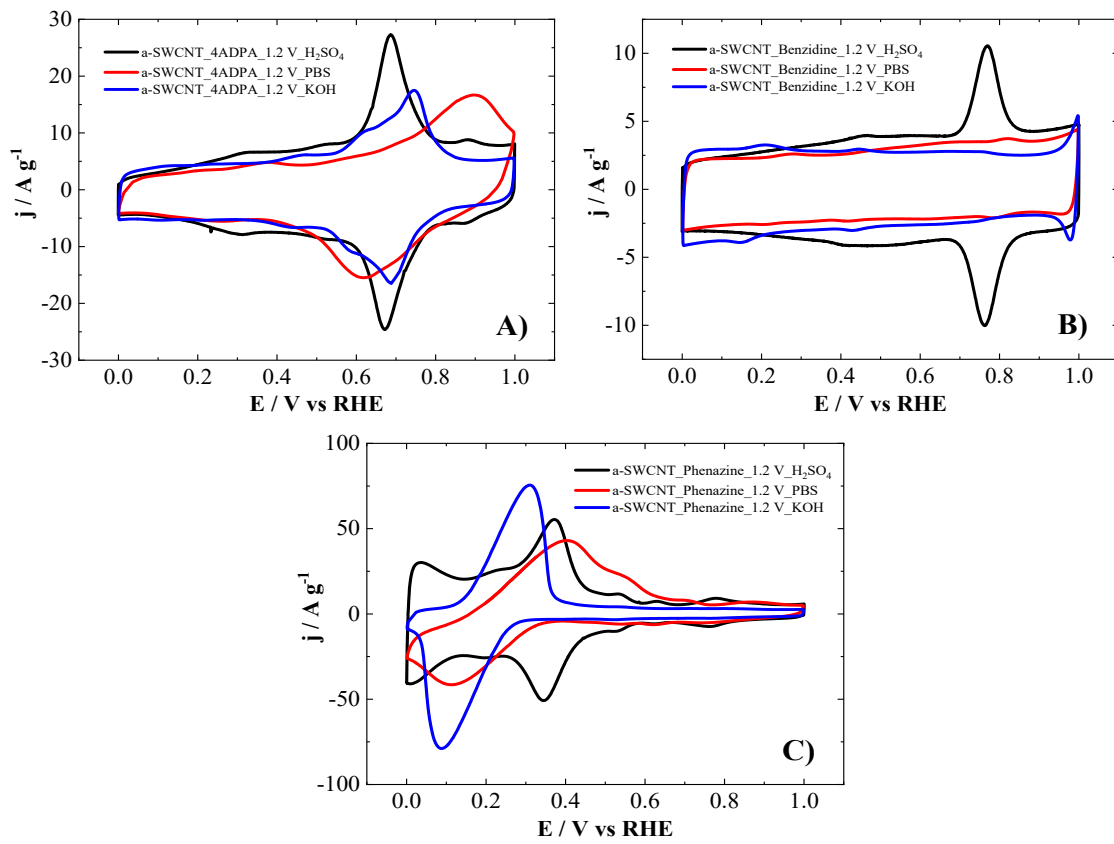


Figure S11. Cyclic voltammograms for a-SWCNT electrochemically modified at 1.2 V (vs RHE) with A) 1 mM 4ADPA, B) 1 mM benzidine and C) 1 mM phenazine, in acid (0.5 M H_2SO_4 , black lines), neutral (0.1 M PBS, pH=7.2, red lines) and alkaline (0.1 M KOH, blue lines) solution free of monomers at 50 mV s^{-1} under N_2 atmosphere. 10th cycle.

Electrochemical studies in presence of 2APPA and 4APPA (0.5 M H₂SO₄ + 1 mM 2/4APPA) were performed by cycling voltammetry and increasing the upper positive potential to higher values from 0.80 to 1.8 V. The stepwise potentiodynamic process in Figure S12 confirms the presence of phosphonic moieties, since the electrochemical response show some changes with respect to the previous study with aniline (Figure 2 in the main text). Moreover, the position of the phosphonic groups seems to be of great relevance for the resultant polymer formation and functionalization.

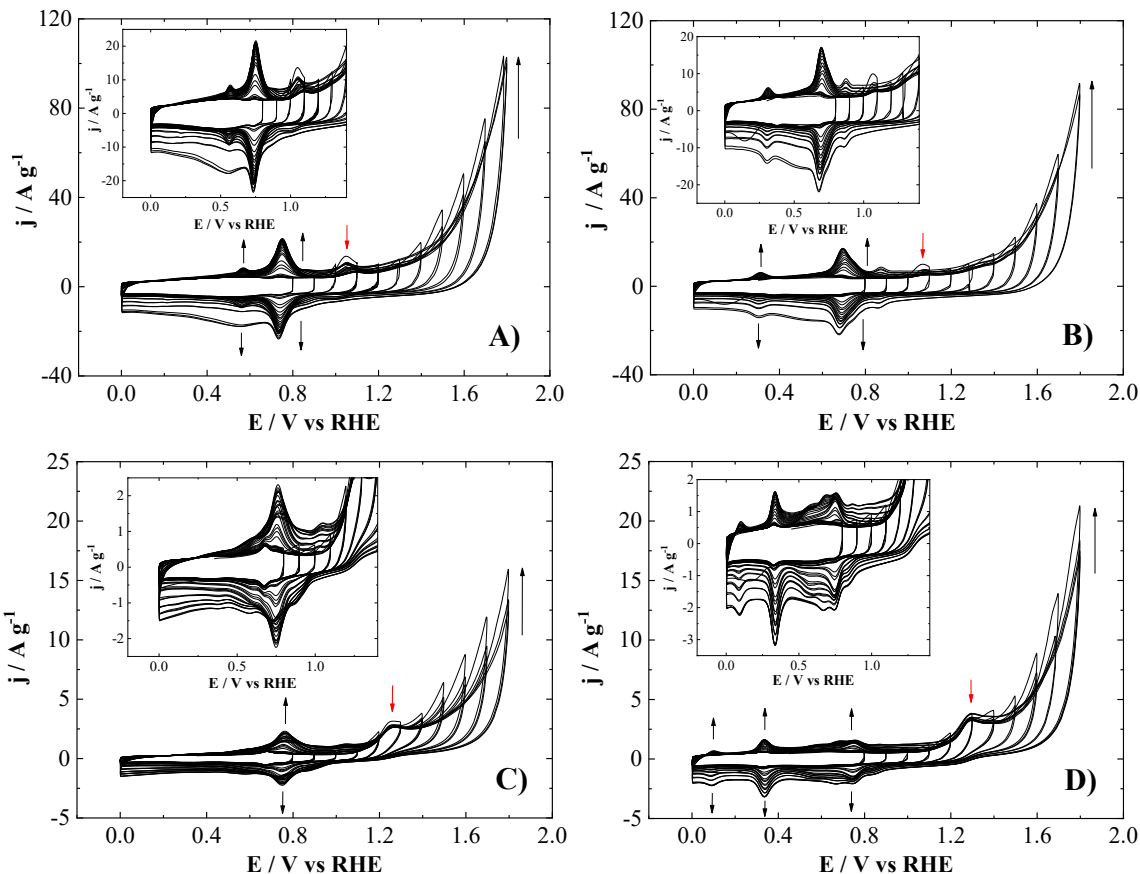


Figure S12. Cyclic voltammograms of the open stepwise upper potential limit from 0.80 to 1.8 V for A, B) a-SWCNT and C, D) hCNT, in 0.5 M H₂SO₄ + A, C) 1 mM 2APPA and B, D) 1 mM 4APPA (right) at 50 mV s⁻¹.

Cyclic voltammograms shown in Figure S12 reveal similar electrochemical responses at low upper potential limits to those observed in presence of aniline. When the potential window is opened to 1.0-1.1 V, an oxidation current appears both for 2APPA and 4APPA (Figure S12A and B) with a-SWCNTs, resembling those observed previously in presence of ANI (Figure 3A in the main text). It is also found that for hCNTs the oxidation peak is

shifted to 1.25 V for 2APPA and 1.30 V for 4APPA (Figure S12C and D, respectively). Therefore, it is expected that the anodic peak corresponds to the oxidation of the amino group present in APPA monomers, followed by radical coupling [1], or the anchoring of C-N species on CNTs surface [2,3]. It is noteworthy the influence of the effective surface area and chemical nature of the electrode on the interaction, growth and quality of stable polymeric materials and/or functionalization. In this sense, a-SWCNTs facilitates the oxidation of APPA monomers, showing lower potential onsets than those obtained over a Pt electrode [4]. Besides, the homopolymerization of 2APPA and 4APPA on Pt electrode is not produced and it requires the presence of aniline to promote the phosphonation of the polyaniline backbone during the electrooxidation. Interestingly, homopolymerization of 2APPA and 4APPA is possible onto CNTs, possibly as result of the interaction between the monomer/polymer-chain and the conjugated structure of SWCNTs and MWCNTs favouring the correct orientation and adsorption of APPA molecule, in comparison with the Pt electrode [3–6].

After the first sweep up to 1.1 V, a decrease of the monomer oxidation peak along with the development of several redox processes occur with the number of cycles, which depend on the APPA monomer employed and the surface chemistry of the CNTs. New redox processes are generated in addition to those observed in Figure 2 (in the main text) for ANI, thus verifying the presence of electroactive species related to phosphonic groups. Specifically, the electrooxidation of a-SWCNTs in presence of 2APPA results in two main oxidation/reduction peaks at 0.56 and 0.75 V. In the same way, the oxidation in presence of 4APPA originates different redox processes at 0.31 and 0.68 V [3], in addition to the process at 0.87 V, which appears less overlapped than for 2APPA. As seen before, the cyclic voltammograms with hCNTs show more notable differences with the appearance of new redox processes in addition to those mentioned above, which are a consequence of their heterogeneity and different structure compared to SWCNTs. For instance, hCNTs modified with 2APPA also show redox peaks at 0.68 and 1.05 V, while 4APPA generates further processes at 0.10 and 0.75 V.

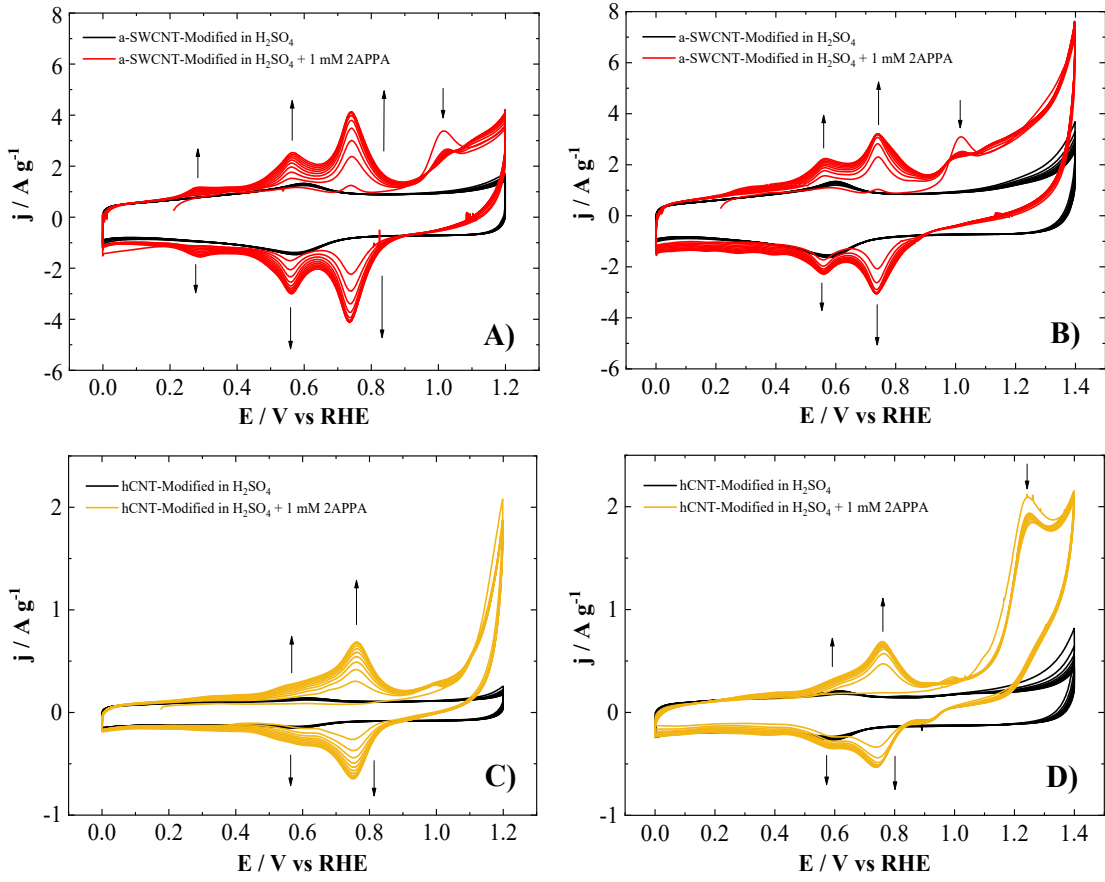


Figure S13. Cyclic voltammograms of the electrochemical functionalization of A, B) a-SWCNT and C, D) hCNT in $0.5 \text{ M H}_2\text{SO}_4$ (black lines) and $0.5 \text{ M H}_2\text{SO}_4 + 1 \text{ mM 2APPA}$ (colored lines) at A, C) 1.2 V and B, D) 1.4 V , at 10 mV s^{-1} under N_2 atmosphere.

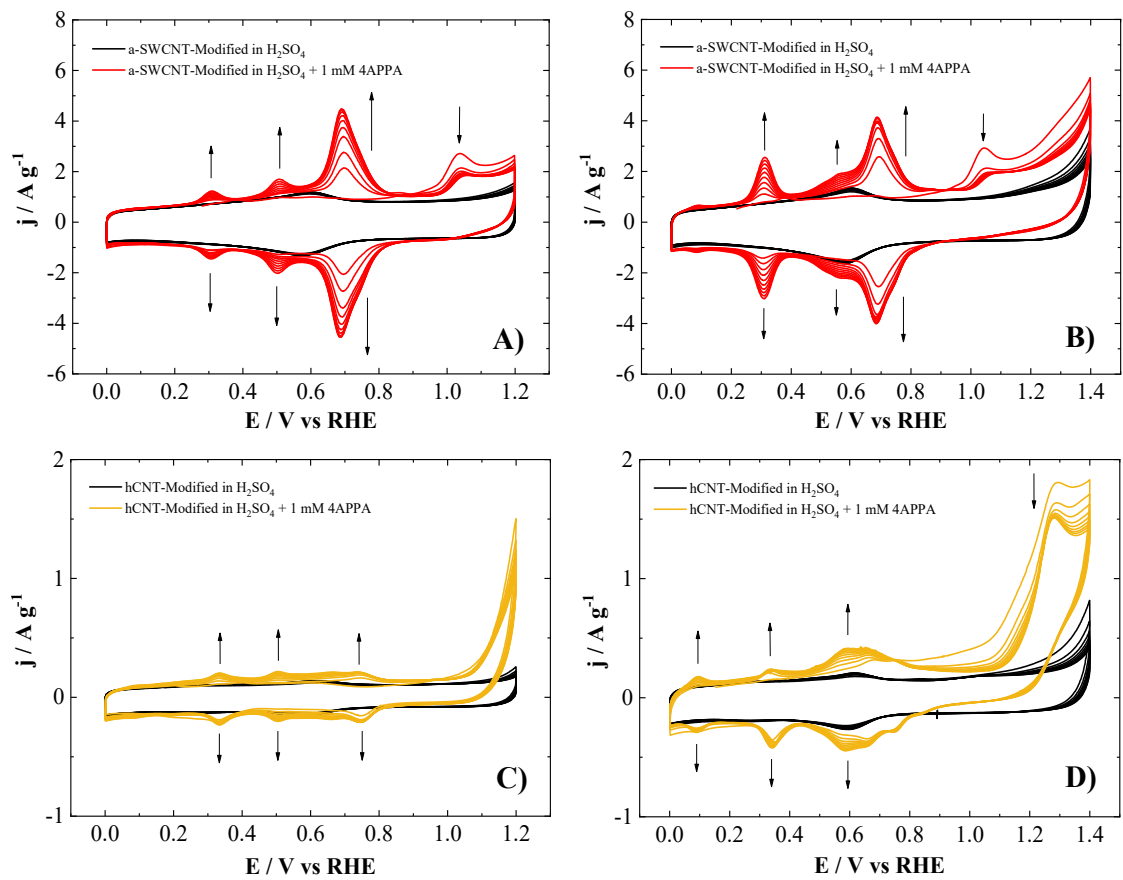


Figure S14. Cyclic voltammograms of the electrochemical functionalization of A, B) a-SWCNT and C, D) hCNT in 0.5 M H_2SO_4 (black lines) and 0.5 M $\text{H}_2\text{SO}_4 + 1 \text{ mM 4APPA}$ (colored lines) at: A, C) 1.2 V and B, D) 1.4 V, at 10 mV s^{-1} under N_2 atmosphere.

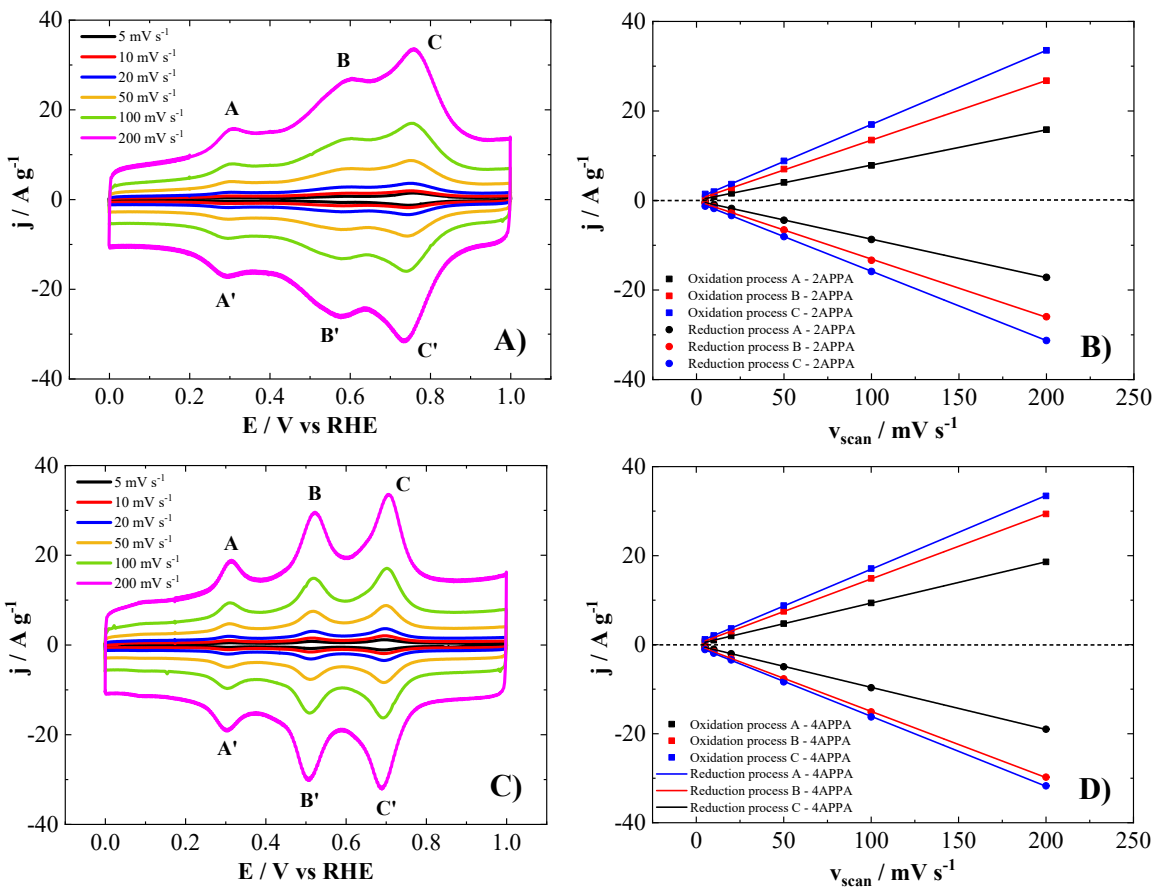


Figure S15. Cyclic voltammograms for a-SWCNT electrochemically modified at 1.2 V (vs RHE) with A) 1mM 2APPA and C) 1 mM 4APPA, at different v_{scan} (5, 10, 20, 50, 100 and 200 mV s⁻¹) in 0.5 M H₂SO₄ under N₂ atmosphere. Correlation of anodic and cathodic current of processes A, B and C vs. v_{scan} generated with B) 2APPA and D) 4APPA, respectively.

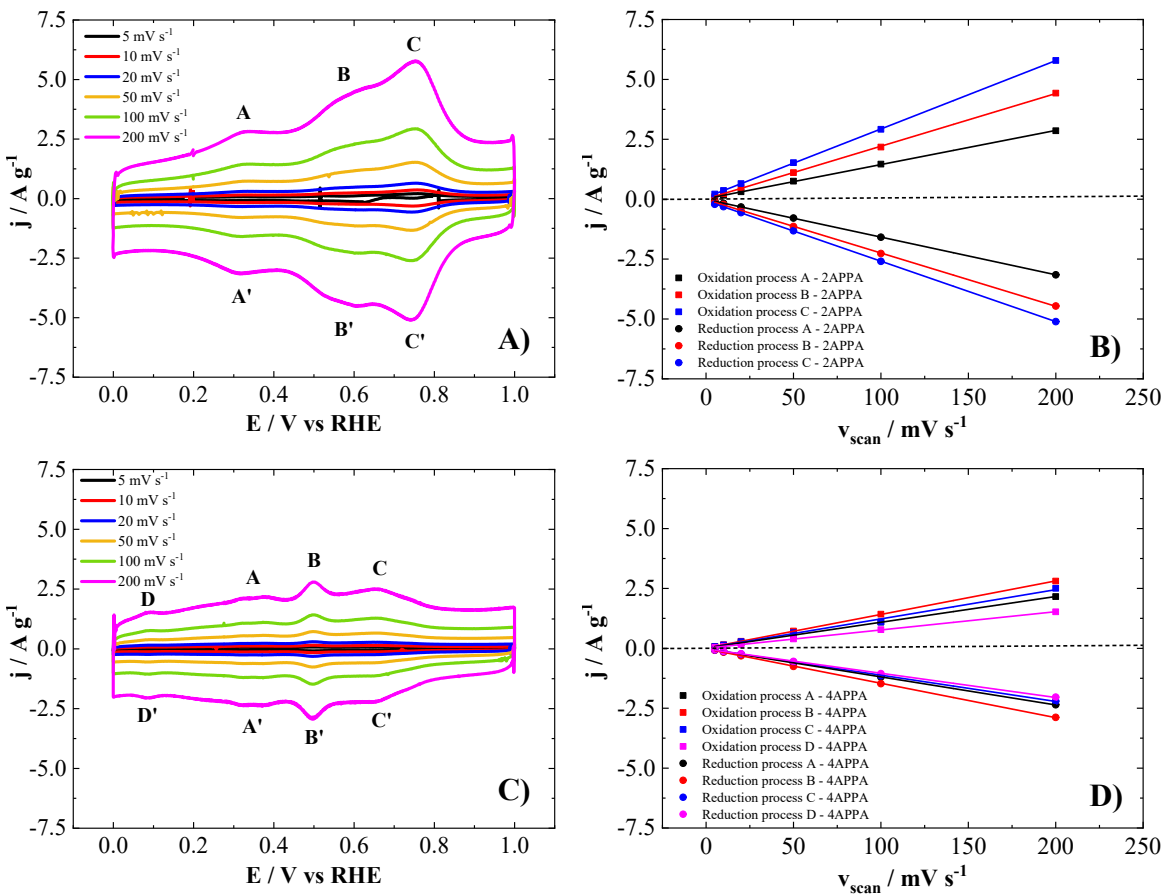


Figure S16. Cyclic voltammograms for hCNT electrochemically modified at 1.2 V (vs RHE) with A) 1 mM 2APPA and C) 1 mM 4APPA, at different v_{scan} (5, 10, 20, 50, 100 and 200 mV s^{-1}) in 0.5 M H_2SO_4 under N_2 atmosphere. Correlation of anodic and cathodic current of processes A, B and C vs. v_{scan} generated with B) 2APPA and D) 4APPA, respectively.

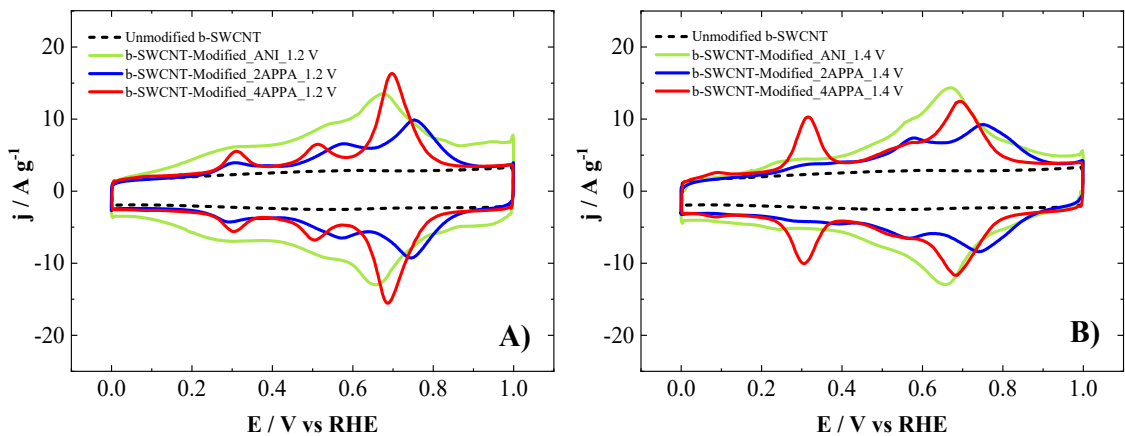


Figure S17. Cyclic voltammograms of b-SWCNT unmodified (dashed lines) and electrochemically modified at A) 1.2 V and B) 1.4 V (vs RHE) with 1 mM ANI (green lines), 1 mM 2APPA (blue lines) and 1 mM 4APPA (red lines), in acid medium (0.5 M H_2SO_4) free of monomers at 50 mV s^{-1} under N_2 atmosphere. 10th cycle.

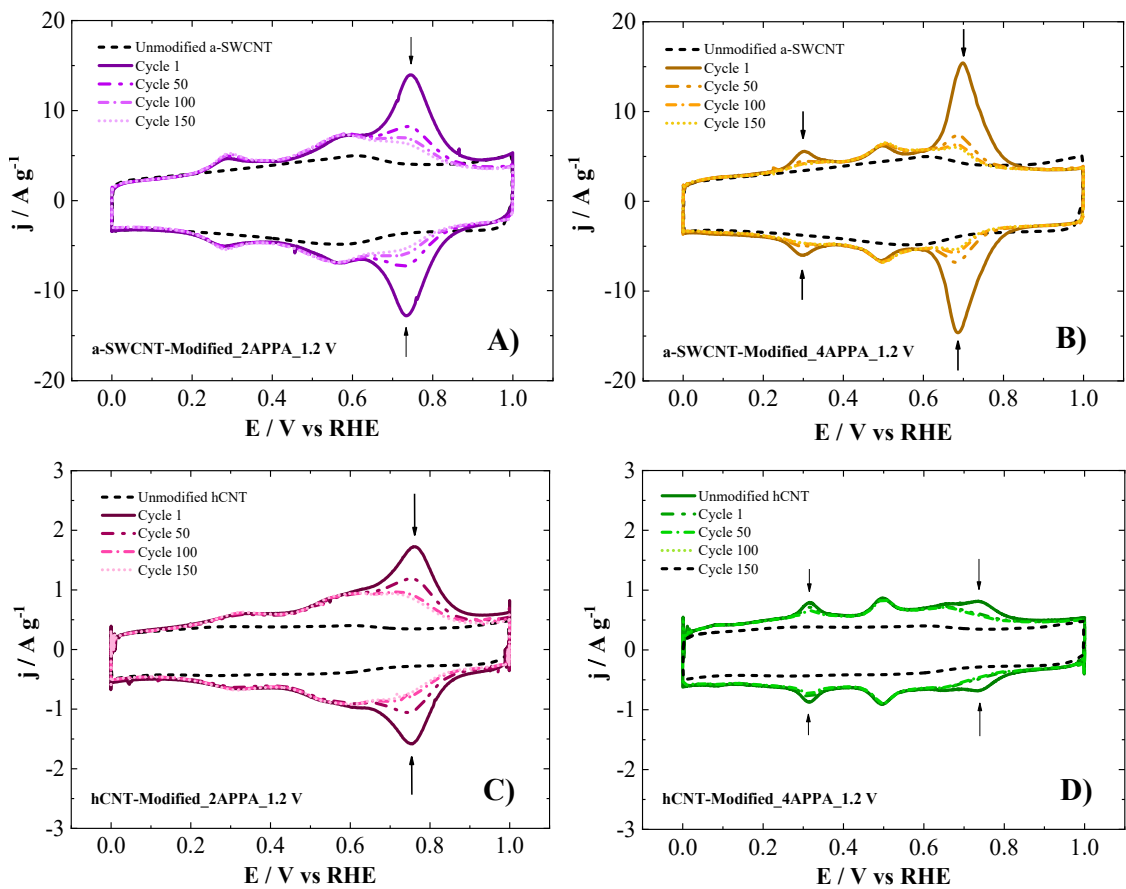


Figure S18. Cyclic voltammograms for A, B) a-SWCNT and C, D) hCNT electrochemically modified at 1.2 V (vs RHE) with A, C) 1 mM 2APPA and B, D) 1 mM 4APPA, in acid solution (0.5 M H_2SO_4) free of monomers at 50 mV s⁻¹ under N_2 atmosphere. Stability test during 150 cycles.

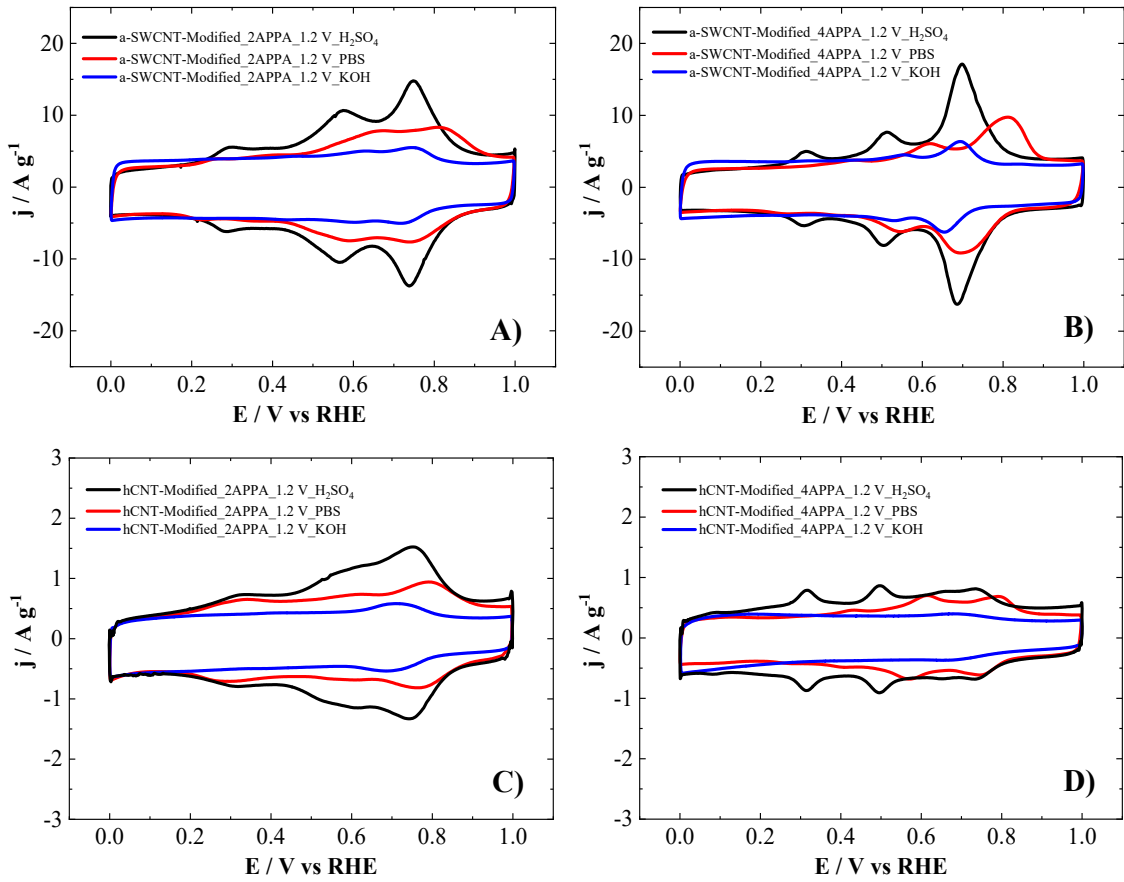


Figure S19. Cyclic voltammograms for A, B) a-SWCNT and C, D) hCNT electrochemically modified at 1.2 V (vs RHE) with A, C) 1 mM 2APPA and B, D) 1 mM 4APPA, in acid (0.5 M H_2SO_4 , black lines), neutral (0.1 M PBS, pH=7.2, red lines) and alkaline (0.1 M KOH, blue lines) solution free of monomers at 50 mV s^{-1} under N_2 atmosphere. 10th cycle.

Table S3. Gravimetric capacitance of a-SWCNT and hCNT, before and after electrochemical functionalization in different pH solutions.

Sample	C / F g ⁻¹ *		
	0.5 M H ₂ SO ₄	0.1 M PBS	0.1 M KOH
a-SWCNT	63	57	58
a-SWCNT_1.2	60	50	52
a-SWCNT_ANI	175	161	162
a-SWCNT_2APPA	127	101	81
a-SWCNT_4APPA	107	86	75
hCNT	7	3	6
hCNT_1.2	8	3	7
hCNT_ANI	26	22	19
hCNT_2APPA	14	12	8
hCNT_4APPA	12	9	7

* The gravimetric capacitance was determined from 0.0 to 1.0 V (vs RHE) at 50 mV s⁻¹, cycle 10.

Table S4. Estimated amount of introduced functionalities on the CNTs modified at 1.2 V with ANI, 2APPA and 4APPA monomers.

	ANI / mmol g⁻¹	2APPA /mmol g⁻¹	4APPA /mmol g⁻¹
a-SWCNT	1.194	0.698	0.485
hCNT	0.181	0.066	0.038

Table S5. Mol percentages estimated from active species determined by cyclic voltammetry on the CNTs modified at 1.2 V with 2APPA and 4APPA monomers.

	2APPA /mol.%	4APPA / mol.%
a-SWCNT	0.98	0.68
hCNT	0.09	0.05

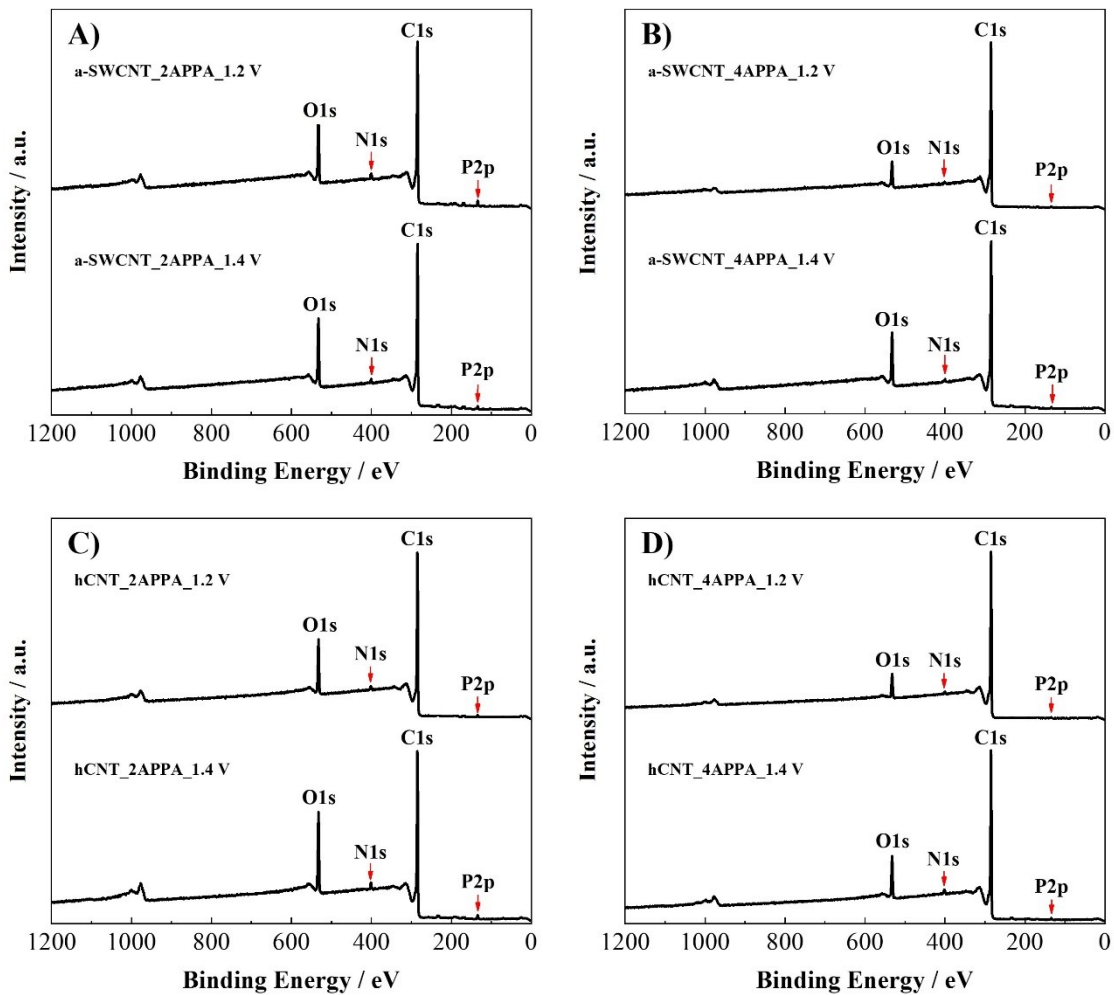


Figure S20. XPS full survey spectra of A, B) a-SWCNT and C, D) hCNTs modified with A, C) 2APPA and B, D) 4APPA at 1.2 V and 1.4 V (vs RHE).

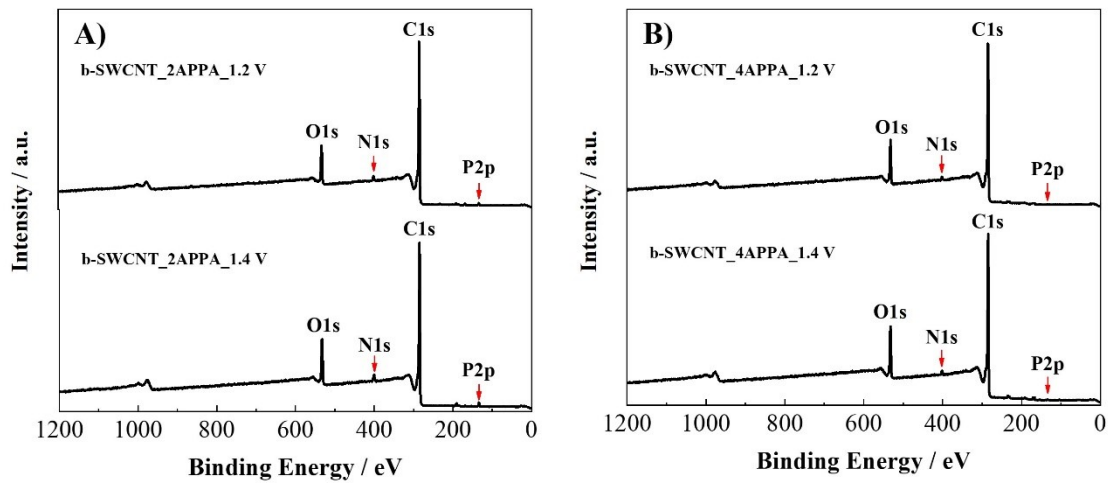


Figure S21. XPS full survey spectra of b-SWCNT modified with A, C) 2APPA and B, D) 4APPA at 1.2 V and 1.4 V (vs RHE).

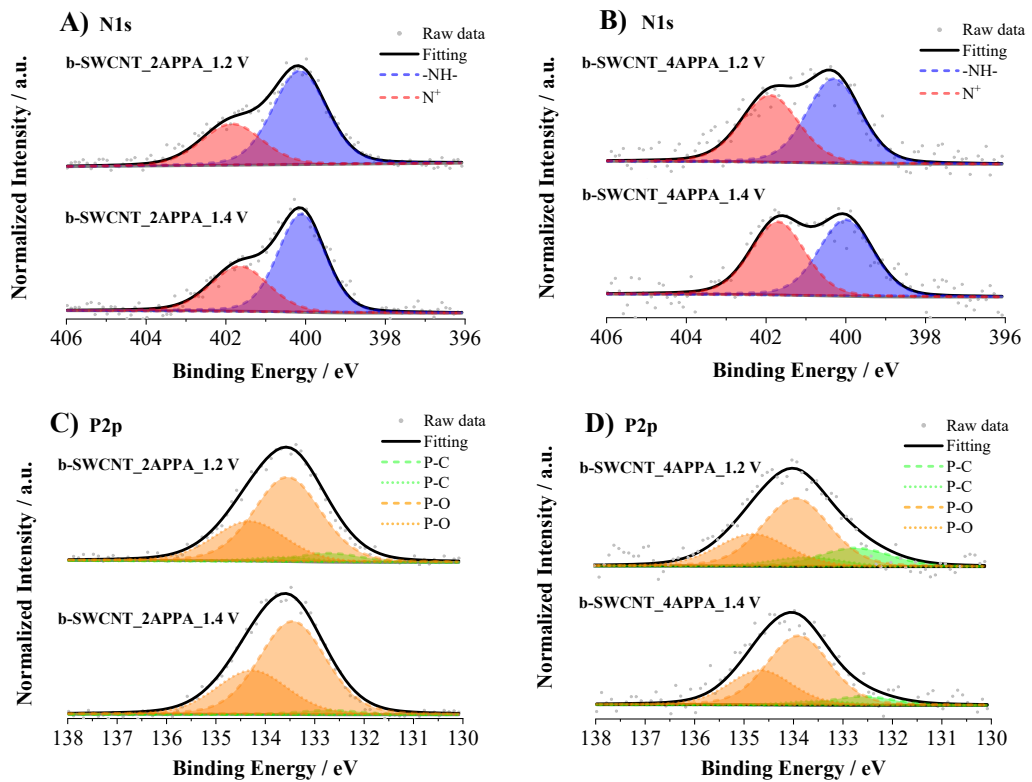


Figure S22. XPS spectra of A, B) N1s and C, D) P2p of b-SWCNT modified with A, C) 2APPA and B, D) 4APPA at 1.2 V and 1.4 V (vs RHE).

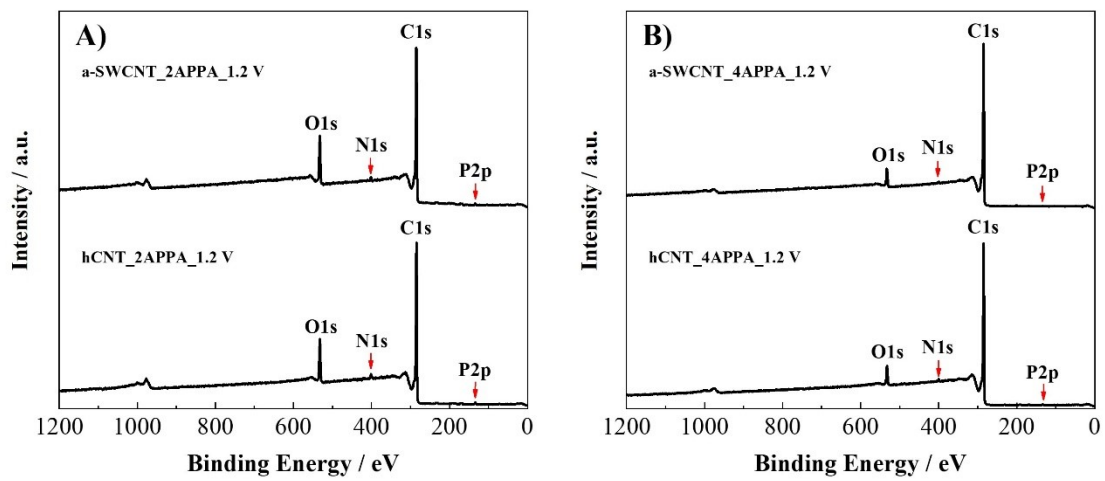


Figure S23. XPS full survey spectra of a-SWCNT and hCNT modified with A) 2APPA and B) 4APPA at 1.2 V (vs RHE), after stability test by cyclic voltammetry during 150 cycles in acid solution (0.5 M H₂SO₄) free of monomers at 50 mV s⁻¹ under N₂ atmosphere.

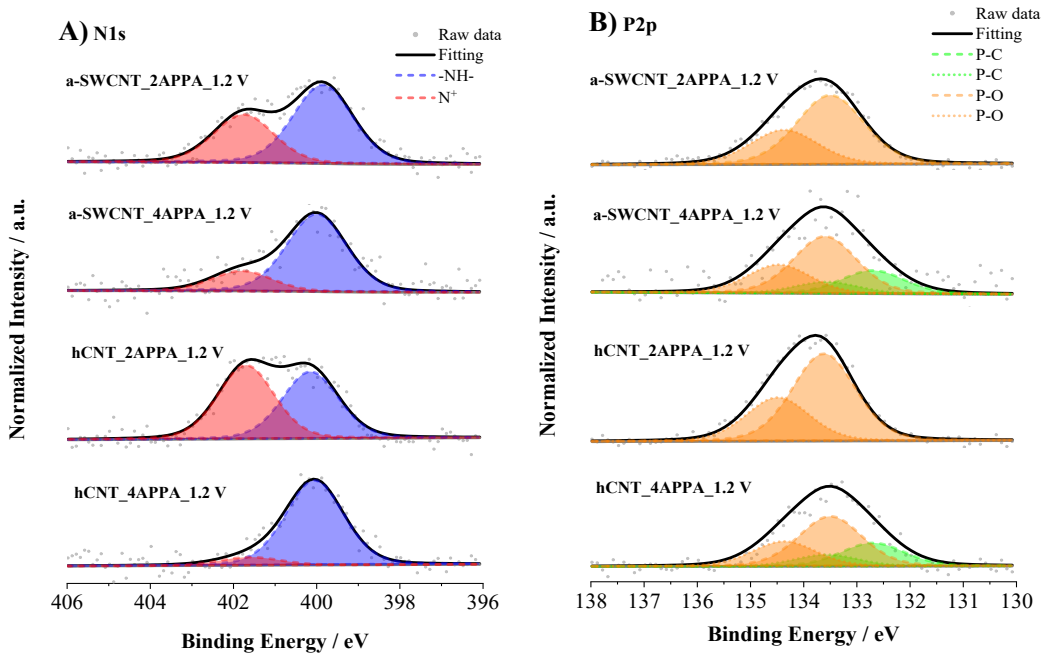


Figure S24. XPS spectra of A) N1s and B) P2p of a-SWCNT and hCNT modified with 2APPA and 4APPA at 1.2 V (vs RHE), after stability test by cyclic voltammetry during 150 cycles in acid solution (0.5 M H₂SO₄) free of monomers at 50 mV s⁻¹ under N₂ atmosphere.

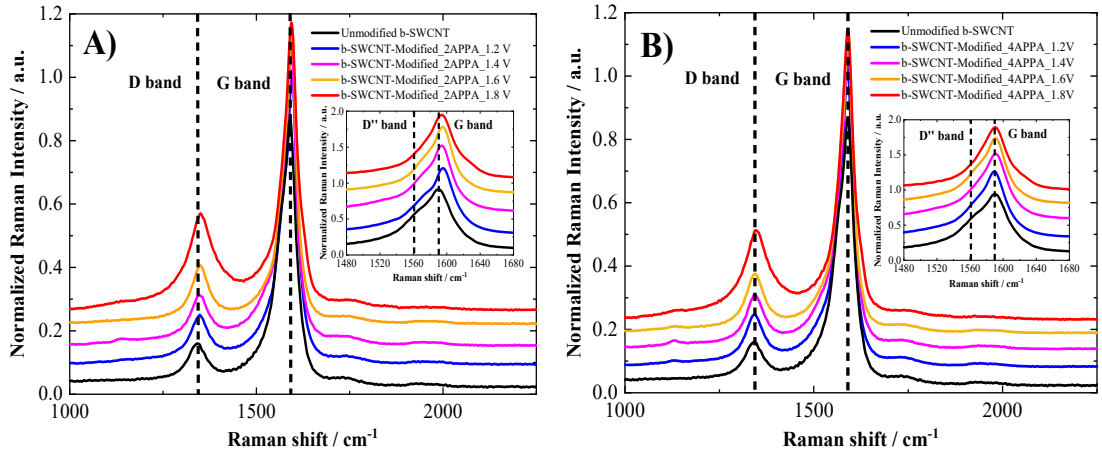


Figure S25. Raman spectra of b-SWCNT electrochemically modified with A) 2APPA and B) 4APPA at different positive potentials. Inset: Enlargement of the D'' and G region.

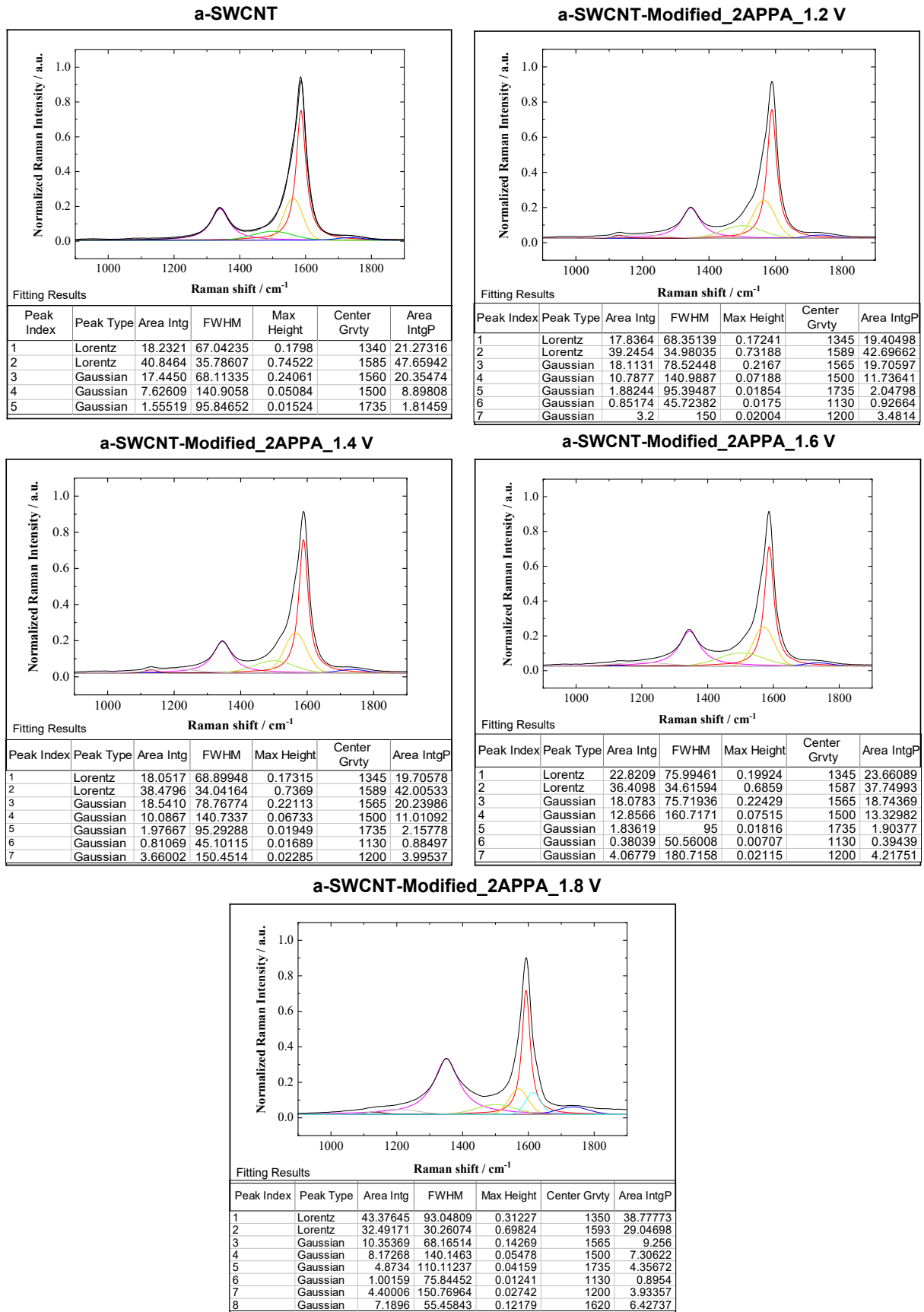


Figure S26. Deconvolution of Raman spectra for a-SWCNT electrochemically modified with 2APPA at different anodic potentials in the D and G region.

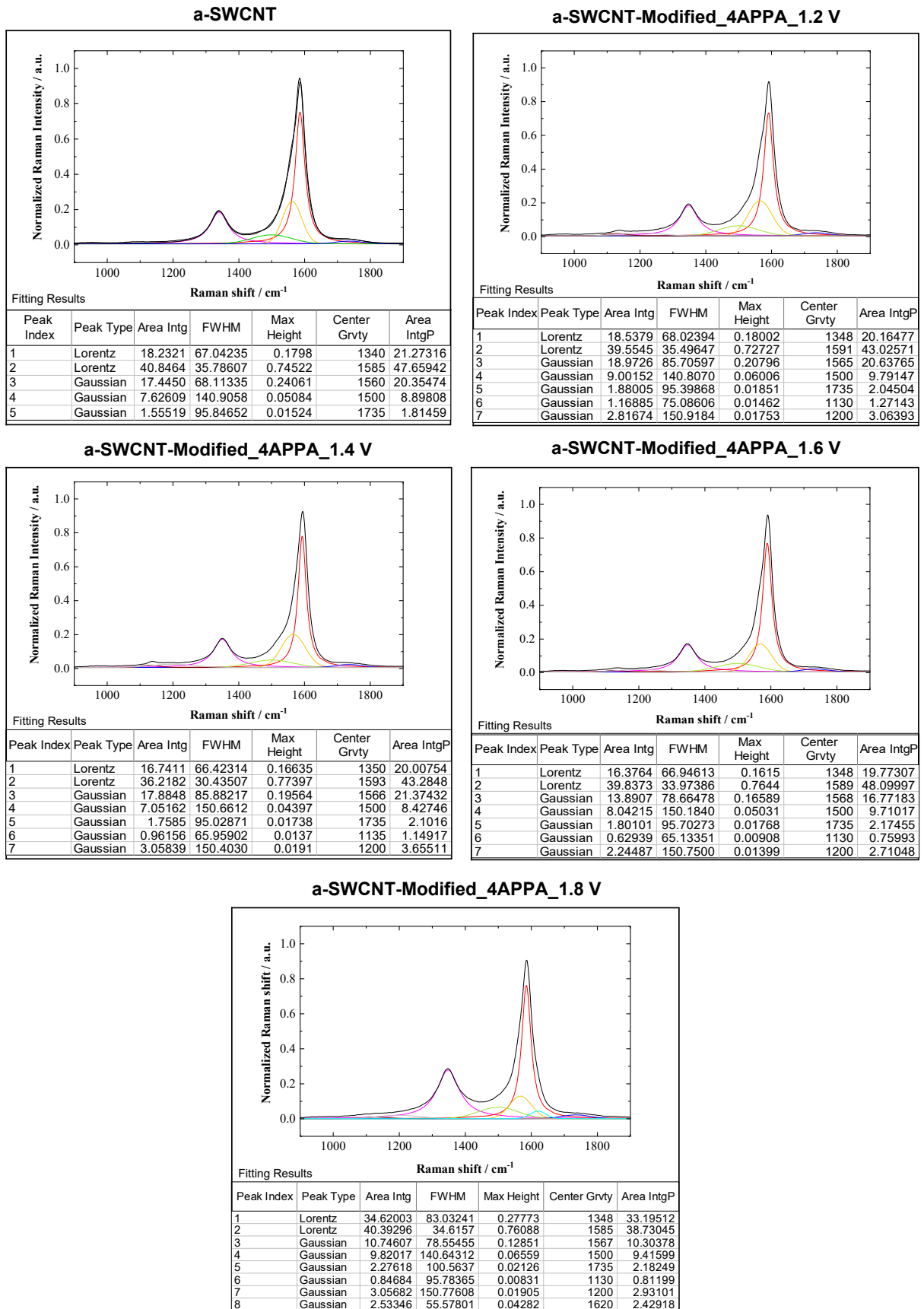


Figure S27. Deconvolution of Raman spectra for a-SWCNT electrochemically modified with 4APPA at different anodic potentials in the D and G region.

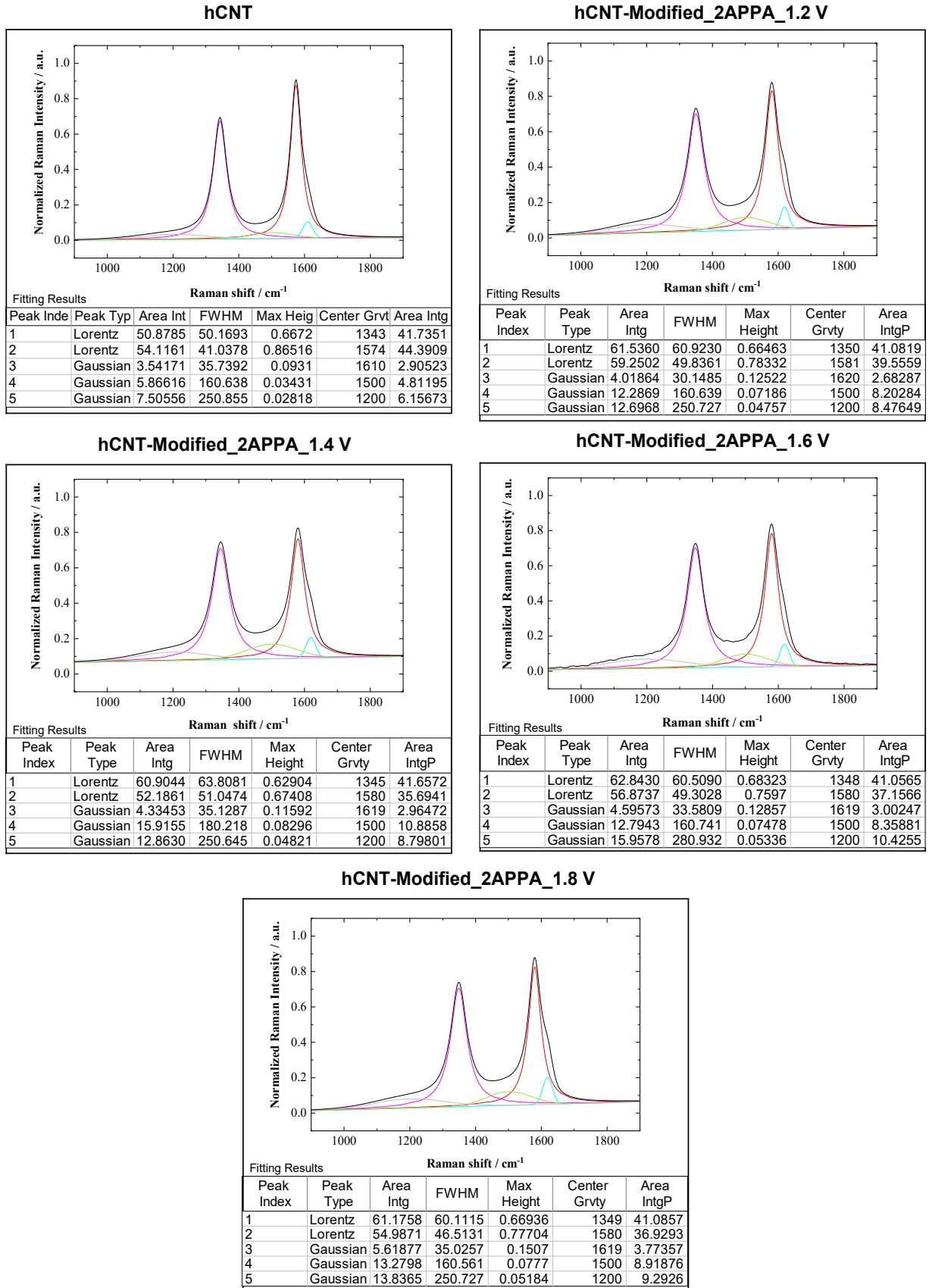


Figure S28. Deconvolution of Raman spectra for hCNT electrochemically modified with 2APPA at different anodic potentials in the D and G region.

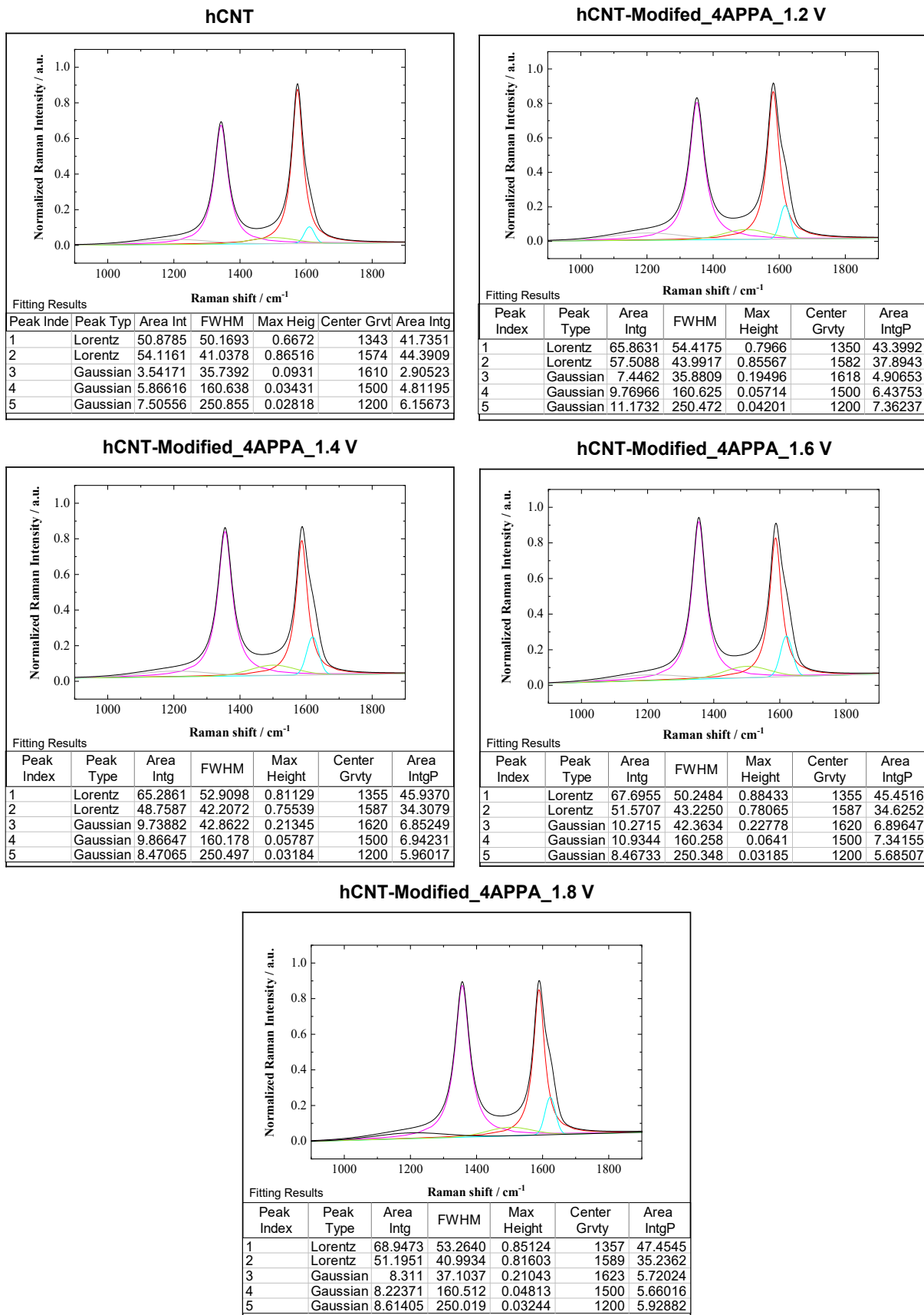


Figure S29. Deconvolution of Raman spectra for hCNT electrochemically modified with 4APPA at different anodic potentials in the D and G region.

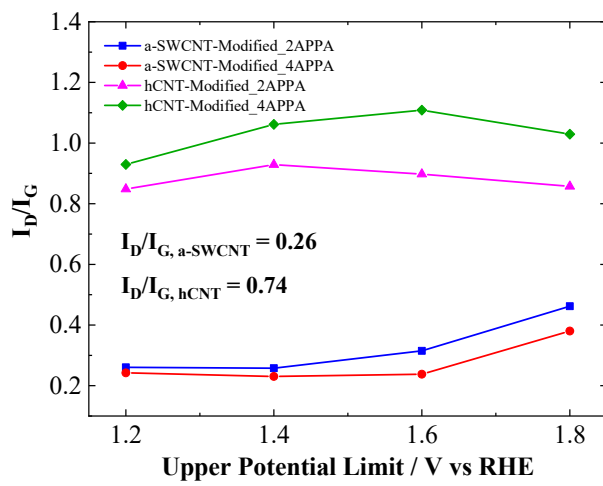


Figure S30. I_D/I_G ratios as a function of the upper potential limit.

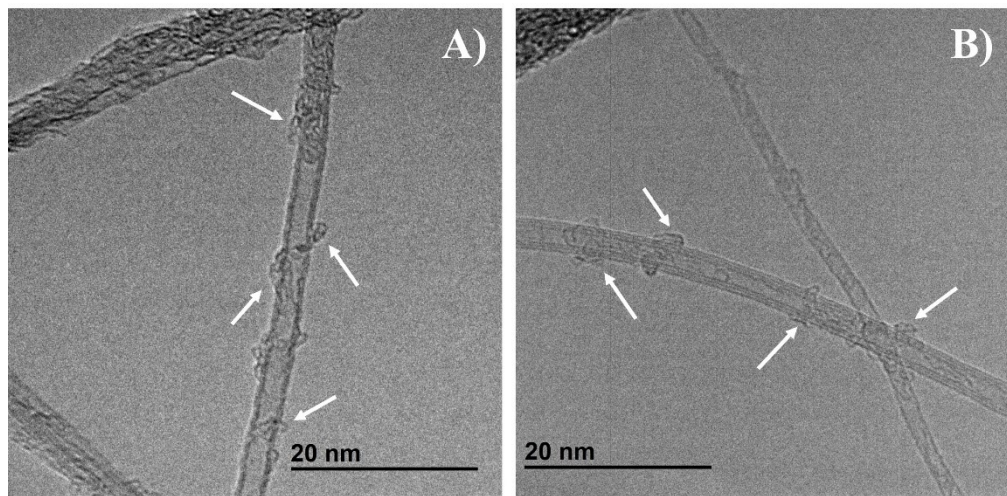


Figure S31. TEM images of b-SWCNT electrochemically modified with A) 2APPA and B) 4APPA at 1.4 V (vs RHE).

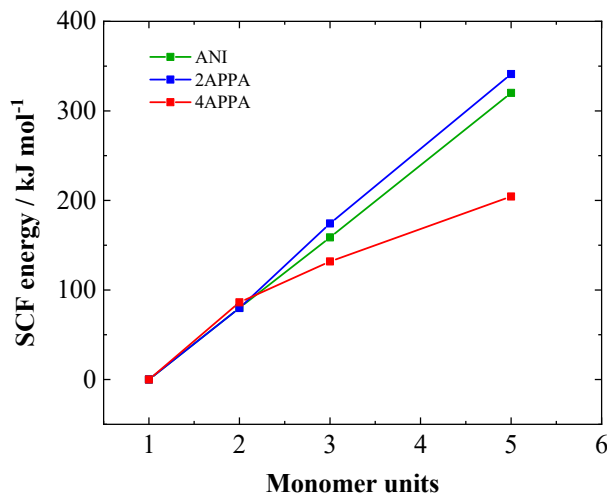


Figure S32. SCF energies of the polymerization for ANI, 2APPA and 4APPA.

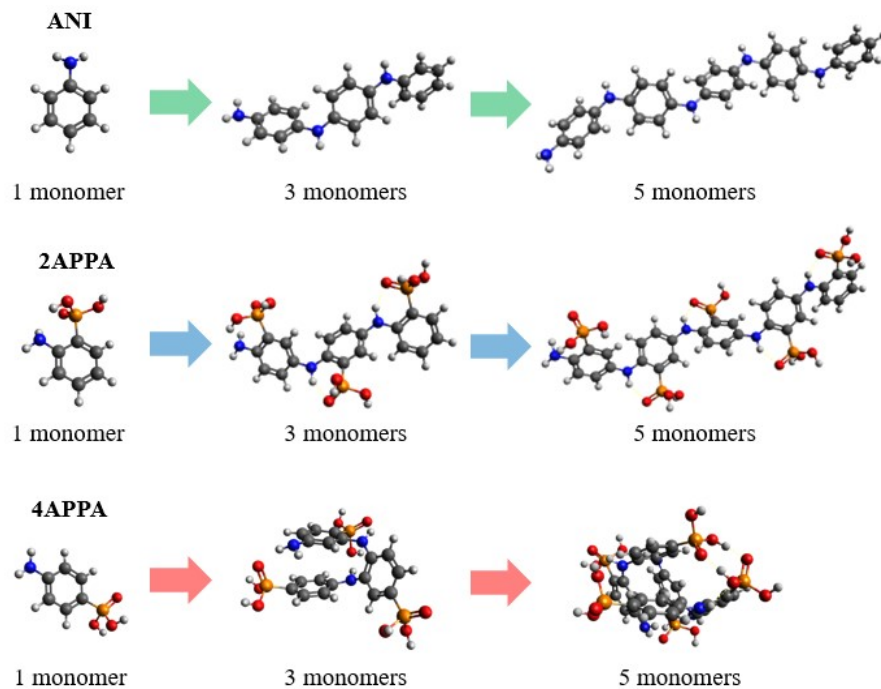


Figure S33. Optimized geometries of the polymerization of 2APPA and 4APPA by using 1, 3 and 5 monomers. H is white, C is grey, N is blue, O is red, and P is orange.

References

- [1] H. Yang, A.J. Bard, The application of fast scan cyclic voltammetry. Mechanistic study of the initial stage of electropolymerization of aniline in aqueous solutions, *J. Electroanal. Chem.* 339 (1992) 423–449.
- [2] C. González-Gaitán, R. Ruiz-Rosas, E. Morallón, D. Cazorla-Amorós, Functionalization of carbon nanotubes using aminobenzene acids and electrochemical methods. Electroactivity for the oxygen reduction reaction, *Int. J. Hydrogen Energy.* 40 (2015) 11242–11253. doi:<https://doi.org/10.1016/j.ijhydene.2015.02.070>.
- [3] A.F. Quintero-Jaime, D. Cazorla-Amorós, E. Morallón, Electrochemical functionalization of single wall carbon nanotubes with phosphorus and nitrogen species, *Electrochim. Acta.* 340 (2020) 135935. doi:<https://doi.org/10.1016/j.electacta.2020.135935>.
- [4] B. Martínez-Sánchez, A.F. Quintero-Jaime, F. Huerta, D. Cazorla-Amorós, E. Morallón, Synthesis of Phosphorus-Containing Polyanilines by Electrochemical Copolymerization, *Polymers.* 12 (2020) 1029. doi:[10.3390/polym12051029](https://doi.org/10.3390/polym12051029).
- [5] C. Downs, J. Nugent, P.M. Ajayan, D.J. Duquette, K.S. V Santhanam, Efficient Polymerization of Aniline at Carbon Nanotube Electrodes, *Adv. Mater.* 11 (1999) 1028–1031. doi:[10.1002/\(SICI\)1521-4095\(199908\)11:12<1028::AID-ADMA1028>3.0.CO;2-N](https://doi.org/10.1002/(SICI)1521-4095(199908)11:12<1028::AID-ADMA1028>3.0.CO;2-N).
- [6] A.F. Quintero-Jaime, D. Cazorla-Amorós, E. Morallón, Effect of surface oxygen groups in the electrochemical modification of multi-walled carbon nanotubes by 4-amino phenyl phosphonic acid, *Carbon.* 165 (2020) 328–339. doi:[10.1016/j.carbon.2020.04.062](https://doi.org/10.1016/j.carbon.2020.04.062).